Journal of Ovonic Research Vol. 5, No. 5, October 2009, p. 145 - 156

SOLID STATE PROPERTIES AND STRUCTURAL CHARACTERIZATION OF Sb_2S_3 AND Tl_2S THIN FILMS

F. I. EZEMA, S. C. EZUGWU*, P.U. ASOGWA, A. B. C. EKWEALOR
Department of Physics and Astronomy, University of Nigeria, Nsukka

Antimony sulphide (Sb_2S_3) and Thallium Sulphide (Tl_2S) thin films each were deposited from aqueous baths on glass substrates. Thin films of antimony sulphide (Sb_2S_3) were deposited from a bath containing antimony trichloride dissolved in acetone and Sodium thiosulphate. Thin films of thallium sulphide (Tl_2S) were deposited from a bath containing thallium nitrate, sodium citrate, sodium hydroxide and thiourea. Some of the films produced were annealed in oven for 2hours at various temperatures. Multilayer films of Sb_2S_3-Tl_2S and Tl_2S-S_2S_3 were also produced, and annealed for 2hours at 180^{o}C. The thin films produced were studied using XRD, spectrophotometer and optical microscope. From the transmittance spectra, the optical band gaps for the films were calculated. The values obtained for these materials are 1.40eV (Sb_2S_3), 1.30eV (Tl_2S) and between 1.40 and 1.70eV for the multilayer films (Tl_2S-Sb_2S_3). Some of the films have very poor transmittance and high absorbance values throughout the solar spectrum and therefore can be used as solar cell absorbers.

(Received Octomber 1, 2009; accepted October 8, 2009)

Keywords: Sb_2S_3, Tl_2Te_3 , Thin films, CBD,Properties, Multilayers, XRD

1. Introduction

For some decades, interest in the binary and ternary chalcogenide thin films has lead to increased research in this area. These thin films have a number of applications in various fields, including coatings, interference filters, polarizers, narrow band filters, solar cells, photoconductors, IR detectors, waveguide coatings, magnetic and superconducting films, microelectronic devices [1,2]. Many metal sulphide compounds have excellent optical properties in the visible and IR region of solar spectrum [3]. Electrical conductivity of thallium sulphide changes with exposure to infrared light, therefore making this compound useful in photocells. The layers of thallium sulphides are commonly produced by the deposition method from solutions [4].

The earlier reports [5-8] of antimony sulphide, is on its applications in microwave devices, switching, television cameras as target materials, and in various optoelectronic devices. Vacuum evaporation techniques [6,9] and chemical bath deposition techniques [10, 11] have been reported for the preparation of thin films of Sb_2S_3. With an optical band gap in the range of 1.06eV to 1.88eV in crystals and in polycrystalline thin films with V_2-VI_3 composition [12], the sulphides of antimony are potential absorber materials in devices for photovoltaic conversion of solar energy. The use of Sb_2S_3 thin films in Schottky barrier solar cells of Pt- Sb_2S_3 [13] and n- Sb_2S_3/p-Ge [14] structures with conversion efficiencies of 5.5 and 7.3 %, respectively, has been reported.

Tl_2S thin film was reported to have an indirect optical band gap of about 1.00eV [15]. Tl_2S-Sb_2S_3 films, which when annealed led to the formation of $TlSbS_2$ with direct band gap of 1.92eV have been reported [16]. Ternary compounds of thallium, which include $TlSbS_2$, have a reported optical band gaps (E_g) of 1.7eV [17] and 1.85eV [18]. Generally optical band gap in the range between 1.00eV and 2.00eV suggests possible application as absorber materials in solar cell.

*Corresponding author: sabro2e@yahoo.com, sabroec@gmail.com

2. Experimental details

The preparations for the deposition of the thins using chemical bath method have been reported by several authors 19-31]

2.1 Deposition of Sb_2S_3 Thin Films

11.51g of $SbCl_3$ was dissolved in 50ml of acetone. 5ml of this solution was placed in a 50ml beaker, to which 12ml of 1.0M sodium thiosulphate and 33ml of distilled water were added. The resulting solution was stirred for a few seconds with glass rod stirrer. A glass slide was inserted in the reaction bath, and held vertically in a synthetic foam cover. This process was repeated for different dip time with various reaction baths.

2.2 Deposition of Thallium Sulphide (Tl_2S) Thin Films

5ml of 0.2 of thallium nitrate ($TlNO_3$) solution were placed in a 100ml beaker, to which 4ml of 1m of sodium citrate and 5ml of 1m sodium hydroxide (NaOH) solutions were added successively. The solution was stirred thoroughly so that a clear homogenous solution was formed. Then 4ml of 1M thiourea solution was mixed and finally 82ml of distilled water was added. The resulting solution, which appears to be black in colours, was stirred for few seconds with a glass rod stirrer before a glass slide was inserted vertically through synthetic foam cover into the solution bath.

2.3 Deposition of Sb_2S_3-Tl_2S and Tl_2S-Sb_2S_3 Thin Films

A sample of deposited Sb_2S_3 was dipped into chemical bath containing starting solutions for deposition of Tl_2S and allowed to deposit on it for few hours after which it was withdrawn, rinsed with distilled water and drip dried, which was considered as Sb_2S_3-Tl_2S. This was annealed in the oven at 180^{o}C for 2hours. The same method was adopted for deposition of Tl_2S-Sb_2S_3. The deposited Tl_2S was dipped in chemical bath for the deposition of Sb_2S_3 and allowed to deposit on the Tl_2S, it was also annealedS for 2hours in an oven

3. Results and discussion

3.1 The Film Structure

The XRD patterns of the crystal nature of the thin films were studied using CuKα radiation source with wavelength 1.54056Å. The scanning were done continuously between 0^o and 70^o at a step size of 0.03 and at time per step of 0.15s on Sb_2S_3, Tl_2S and Tl_2S-Sb_2S_3 thin films deposited onto glass. The XRD result is shown in figure 1. The diffraction peaks that appeared at $2\theta = 27^o$ (100%), 28^o (66%), 31^o (16%), 36^o (68%) and 37^o (45%) correspond to diffraction planes for Sb_2S_3 film. The diffraction peaks at $2\theta = 25^o$ (20%), 27^o (11%) and 37^o (59%) correspond to peaks of Tl_2S. The diffraction peaks at $2\theta = 19^o$ (13%) and 37^o (92%) correspond to peaks of Tl_2S-Sb_2S_3. Fig. 1 confirms the formation of a ternary compound upon annealing of Sb_2S_3-Tl_2S films.

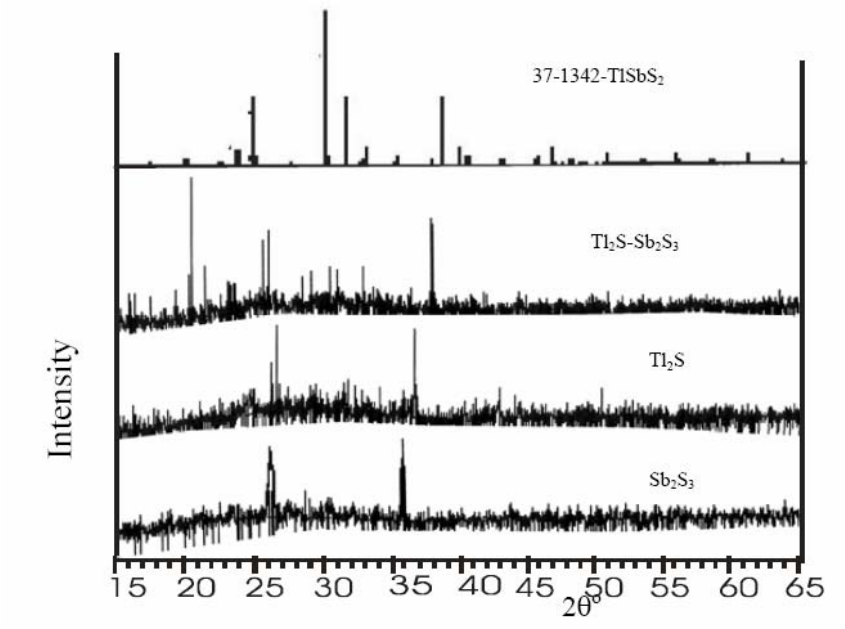

Fig. 1. XRD Pattern for Sb_2S_3, Tl_2S and Tl_2S-Sb_2S_3 Thin Films.

The XRD peaks exhibited by the annealed films match the standard pattern of $TlSbS_2$ (PDF#37-1342). The peak located at $2\theta = 28^{o}$ is ascribed to Sb_2O_3, formed due to hydroxide phase incorporated in the Sb_2S_3 film and Sb_2S_3-Tl_2S interface during the deposition. The photographical structures of the films grown in this work were studied by photomicrograph method with ortholux II photoscope. The photomicrographs of these films are displayed in fig. 2.

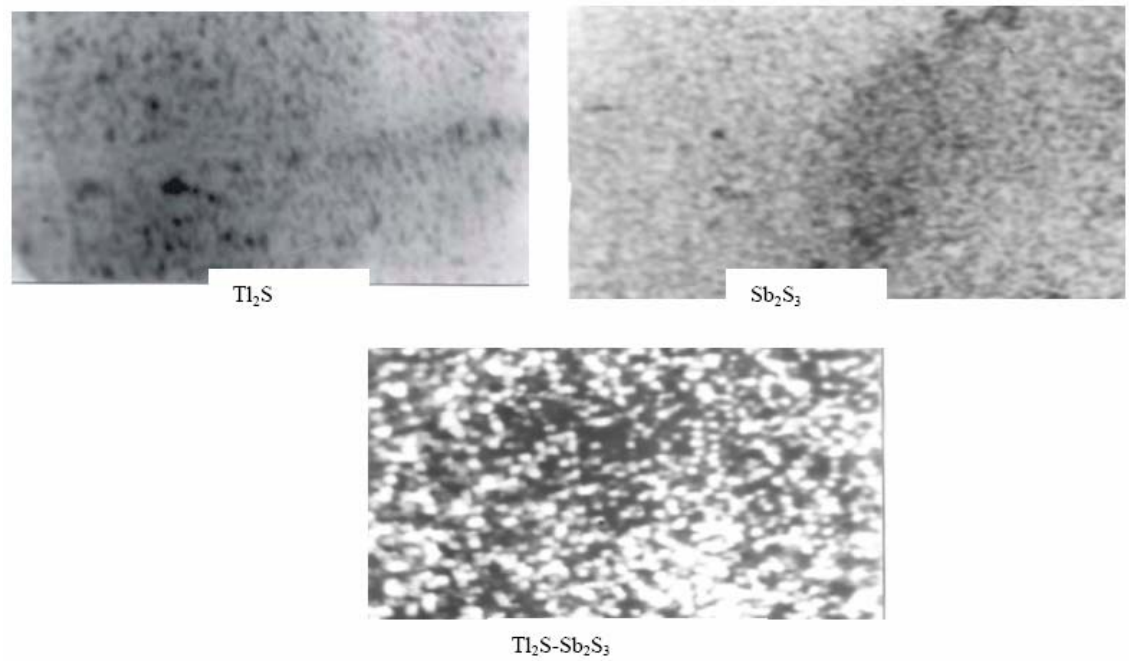

Fig. 2. Optical Micrograph for Sb_2S_3, Tl_2S and Tl_2S-Sb_2S_3 Thin Films (X250).

The structure of the films deposited show that some of the films are crystalline while some show poor crystalline structures. When Tl_2S-Sb_2S_3 was annealed in oven for 2hours at $180^{o}C$ a good crystal structure was observed with optical microscope.

3.2. The transmission of solar radiation

The optical transmittance (T%) and the near-normal specular reflectance spectra (R%) of the films were recorded on a PYE-UNICO UV-2102 PC Spectrophotometer with air and a front aluminized mirror, respectively, as references. Fig. 3 and 4 show the spectral transmission for Sb_2S_3, Tl_2S and Sb_2S_3-Tl_2S films. All the samples show poor transmission of the solar radiation, which indicate high absorption of solar spectrum by the thin films.

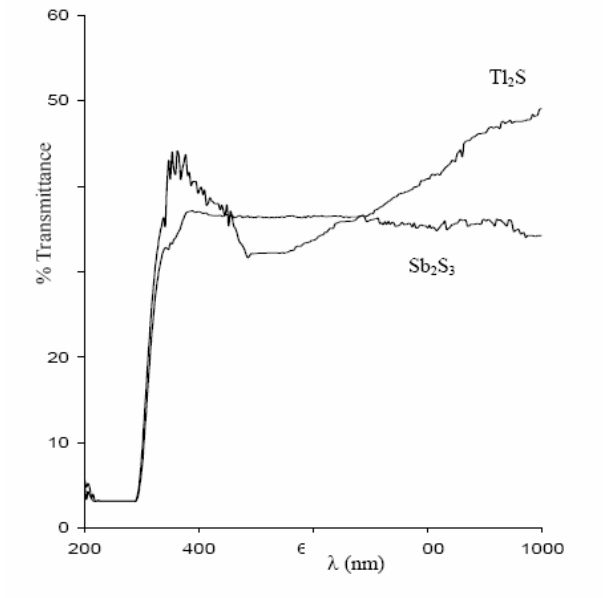

Fig. 3: Transmittance (T) as function of wavelength (λ) for Tl_2S and Sb_2S_3 Thin Films.

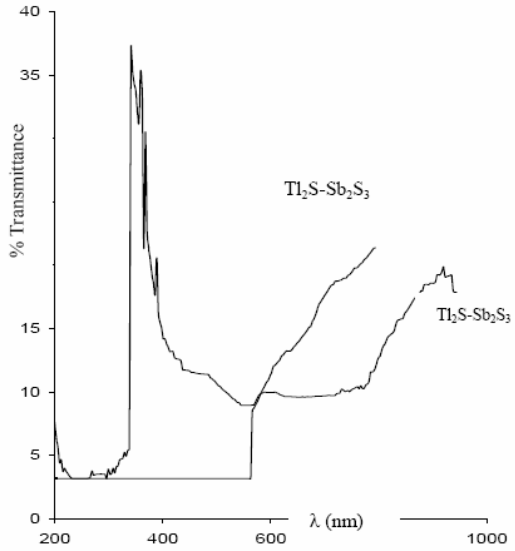

Fig. 4: Transmittance (T) as function of wavelength (λ) for Tl_2S-Sb_2S_3 Thin Films.

The regions of visible-near infrared show poor transmission of solar radiation, which increases from the visible region towards the infrared regions for the samples under consideration

3.3 The optical energy gap

The equation derived for the determination of energy band gap values (E_g) is given as [32-34]

$$\alpha(h\nu) = \frac{A}{h\nu}(h\nu - E_g)^m \quad (1)$$

where m =1/2 for allowed direct transition, m =3/2 for direct ‘‘forbidden’’ transition, m = 2 for allowed indirect transition and m =3 for indirect ‘‘forbidden’’ transition, A is a constant nearly independent on photon energy and known as the disorder parameter. The values of the optical band gap of Sb_2S_3, Tl_2S and Tl_2S-Sb_2S_3 thin films are obtained by plotting $(\alpha h\nu)^{1/m}$ versus hν in the high absorption range followed by extrapolating the linear region of the plots to $(\alpha h\nu)^{1/m} = 0$. The analysis of our data showed that plots of $(\alpha h\nu)^{1/m}$ against hν give a linear relation which is best fitted by equation (1) with m =1/2. This indicates that the allowed direct transition is responsible for interband transition in the films. The plot of $(\alpha h\nu)^2$ against photon energy for the films is represented in Fig. 5 and 6 and, as expected from equation 1, these are linear at the higher values of α(hν) but tend to deviate from linearity at low photon energies.

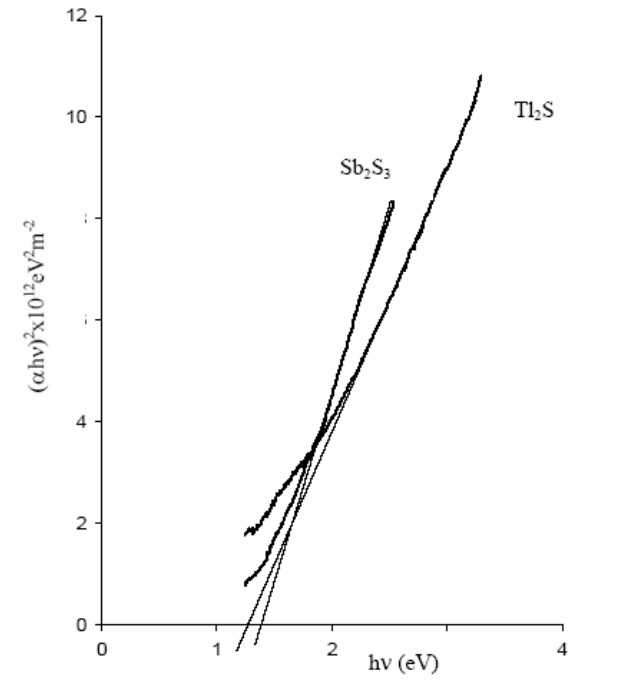

Fig. 5. Plots of $(\alpha h\nu)^2$ as a function of Photon Energy ($h\nu$) for Tl_2S and Sb_2S_3 Thin Films.

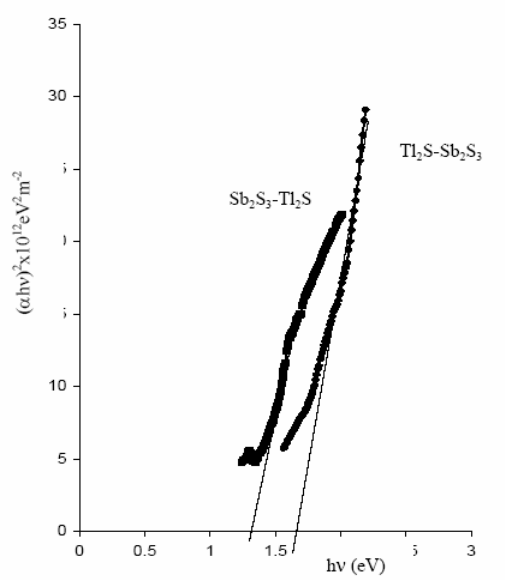

Fig. 6. Plots of $(\alpha h\nu)^2$ as a function of Photon Energy ($h\nu$) for Tl_2S-Sb_2S_3 Thin Films.

These graphs extrapolated to hν axis give the values of E_g as 1.40eV for Sb_2S_3, 1.30eV for Tl_2S, 1.35eV for Sb_2S_3-Tl_2S and 1.70eV for Tl_2S-Sb_2S_3. When Tl_2S-Sb_2S_3 was annealed in oven for 2hours at 180^{o}C a ternary compound $TlSbS_2$ films was produced with band gap of 1.70eV. Compared with the band gap energy of between 1.70 and 2.43eV [12-14] for Sb_2S_3, 1.00eV [16] for Tl_2S and 1.70eV [16,17] for $TlSbS_2$, the band gap energy of the thin films is somewhat reasonable. The variation of the band gap energy was assumed to result from the defects in the thin films, which could be observed in the photomicrograph (fig.2). The obtained films show poor transmission of visible light. There is incorporation of hyroxide phase, clusters and particulate, and growth of monocrystals of a few tens of micrometers diameters over the film surface [31,35]. The influence of factors such as grain size, carrier concentration, crystalline phases present in the sample, presence of impurities, lattice strain, or even deviation from stoichiomtry could be the physical reasons for the discrepancies on the band gap energy obtained in this work and the reported value for E_g in the films.

3.4. Optical constants[33,36-40]

The uses of films in optical applications require accurate knowledge of the optical constants over a wide wavelength range [33,36-40].

3.4.1. Extinction coefficient and refractive index

The reflectivity (R) of materials of refractive index (n) and extinction coefficient (k) is given by [36,37].

$$R = \frac{(n-1)^2+k^2}{(n+1)^2+k^2} \tag{2}$$

The optical transmittance (T) is related to the absorption coefficient (α) and the refractive index (n) by the relation [33]:

$$T = \frac{(1-R)^2 \exp(-\alpha d)}{(1-R^2)\exp(-2\alpha d)} \tag{3}$$

The extinction coefficient (k) is related to α by the relation [33,36]:

$$k = \frac{\alpha\lambda}{4\pi} \tag{4}$$

By these relations, k and n can be defined from the measurements of R and T.
The dielectric constant is related to n and k by the relations [33,36,37]:

$$\varepsilon_r = n^2 - k^2 \tag{5}$$

for real part, and

$$\varepsilon_i = 2nk \tag{6}$$

for imaginary part

The variation of the extinction coefficient k and imaginary part of the dielectric constant ε_i with photon energy for the films are shown in Figs. 8 and 9 respectively.

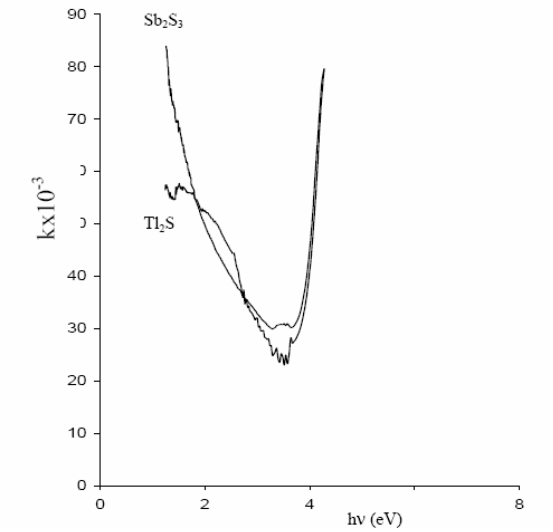

Fig. 8: Variation of the extinction coefficient k with photon energy for Tl_2S and Sb_2S_3 Thin Films.

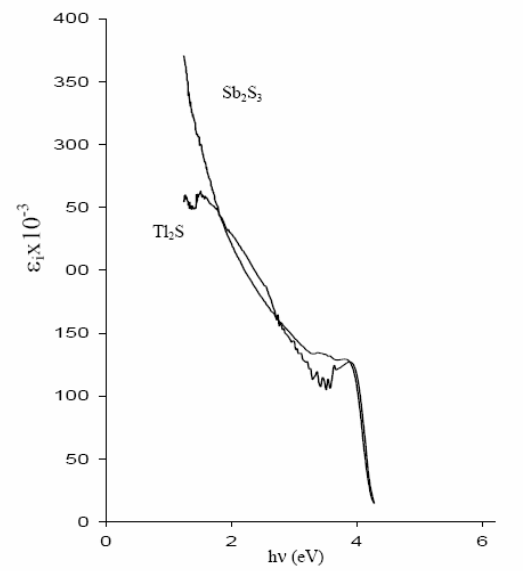

Fig. 9. Variation of the imaginary part of the dielectric constant ε_i with photon energy for Tl_2S and Sb_2S_3 Thin Films.

From these figures we can see that the imaginary part of the dielectric constant increases as the photon energy decreases. The extinction coefficient k decreases with decreasing photon energy to a minimum and increases with decreasing photon to a maximum value in Sb_2S_3 and Tl_2S films.

The dependence of the real part of dielectric constant and that of refractive index on photon energy is shown in Figs. 10 and 11 for the films. It can be noted from these figures that the refractive index and real part of dielectric constant increase with the decreasing photon energy but flattens for Tl_2S films at the lower energy regions.

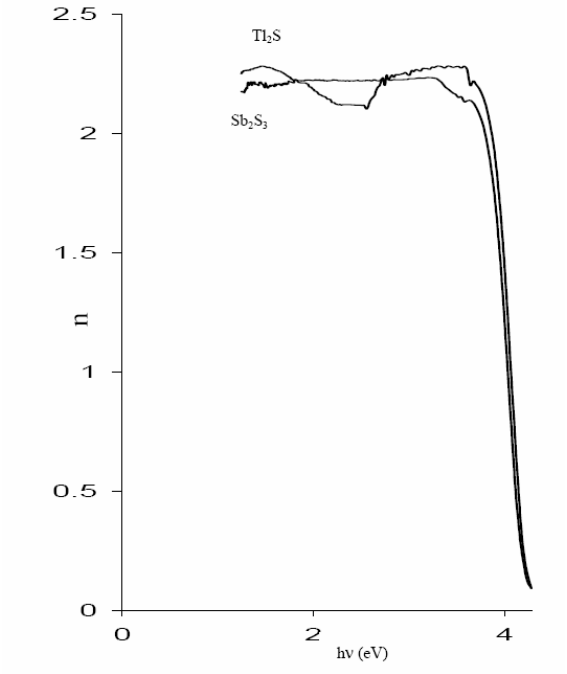

Fig. 10: Variation of the refractive index with photon energy photon energy Tl_2S and Sb_2S_3 Thin Films.

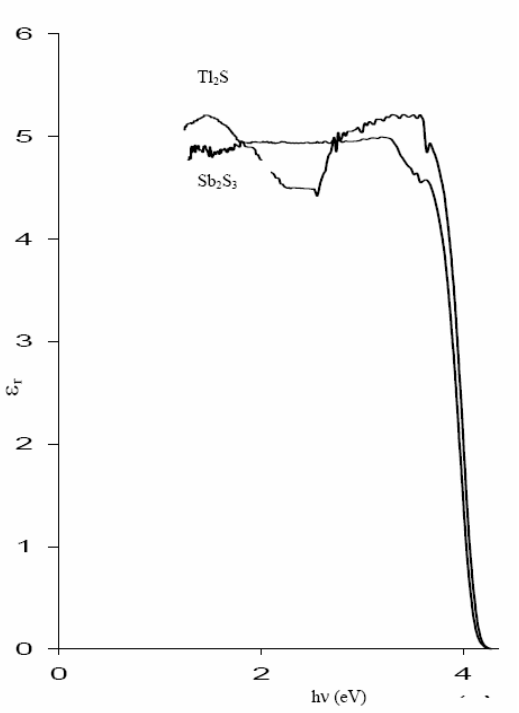

Fig. 11: Variation of the real part of dielectric constant with for Tl_2S and Sb_2S_3 Thin Films.

Figs. 10 and 11 show that the refractive index exhibits a significant dispersion in the short wavelength region below λ= 356nm (3.51 eV) where absorption is strong. It decreases with the increase of the energy of the incident light, becoming nearly flat in the higher region. It is observed also that n reached a peak value at 1.27 eV for Sb_2S_3 and 1.74 eV for Tl_2S and this peaks occurred more at the same energy in the real part of the dielectric constant (ε_r) energy dependence.

3.4.2. Parameters of the single oscillator model

A single effective oscillator model [38,39] was used to evaluate the data on the spectral dependence of refractive index. The dispersion data for more than 100 different materials, which were both covalent and ionic and both crystalline and amorphous were estimated and the optical data were described to a very good approximation by the following formulae[35]:

$$\varepsilon_r(E) = 1 + \frac{E}{(E_o^2 - E^2)} \tag{7}$$

$$n^2(E) - 1 = \frac{E_d E_o}{(E_o^2 - E^2)} \tag{8}$$

where n is the refractive index, E_o is the energy of the effective dispersion oscillator, E is the photon energy and E_d is the dispersion energy. The latter quantity measures the average strength of interband optical transitions. Plotting $(n^2\text{-}1)^{-1}$ against $(h\nu)^2$ allow us to determine the oscillator parameters by fitting a straight line to the points, as shown in Figs. 12 and 13. The values of E_o and E_d can be determined directly from the slope $(E_oE_d)^{-1}$ and the intercept on the vertical axis, (E_o/E_d). As the single oscillator parameters E_o and E_d are connected to the imaginary part of the complex dielectric constant, the M-1 and M-3 moments of the ε(E) optical spectrum and the refractive

index for long wavelength value (n_∞) according to the relations [35]:

$$E_o^2 = \frac{M_{-1}}{M_{-3}} \tag{9}$$

$$E_d^2 = \frac{M_{-1}^3}{M_{-3}} \tag{10}$$

$$n_\infty^2 - 1 = \frac{E_d}{E_o} \tag{11}$$

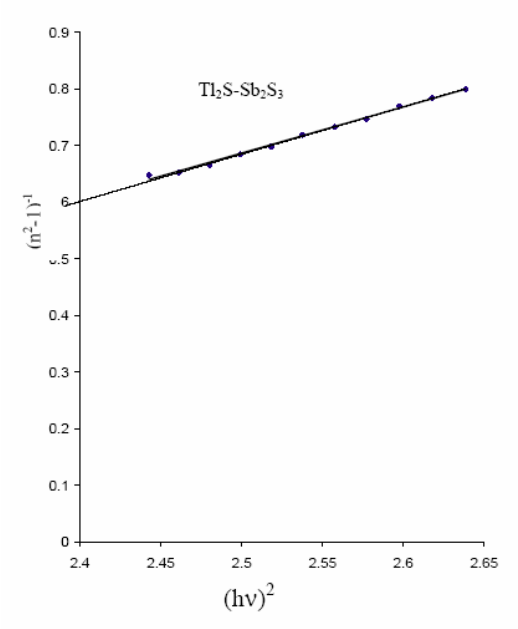

Fig. 12 Plots $(n^2-1)^{-1}$ against $(h\nu)^2$ for Tl_2S and Sb_2S_3 Thin Films.

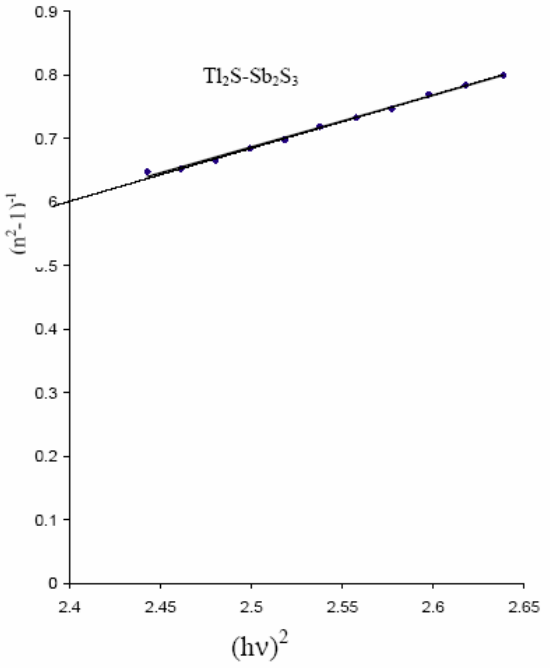

Fig. 13 Plots $(n^2-1)^{-1}$ against $(h\nu)^2$ for Tl_2S-Sb_2S_3 Thin Film.

From Figs. 12 and 13 we can calculate the values of E_o, E_d, M-1, M-3 and n_∞ for the films and these values are listed in Table 1.

Table 1: Optical constants for Sb_2S_3, Tl_2S and Tl_2S-Sb_2S_3 thin films

	E_o	E_d	M-1	M-3	n_∞	E_g (eV)
Tl_2S-Sb_2S_3	3.35	5.59	1.66	0.14	1.63	1.70
Sb_2S_3	2.61	9.70	3.72	0.55	2.17	1.30
Tl_2S	2.85	11.62	4.08	0.50	2.25	1.40

The obtained values strongly agree with Wemple [26] and Wemple and Di Domentic [27]. The single oscillator energy E_o is found to be twice [28,29] the optical energy gap E_g. This is reasonably supported and fairly agrees with our result.

4. Conclusions

Thin films of Sb_2S_3, Tl_2S and Tl_2S-Sb_2S_3 were successfully deposited using chemical bath deposition method. On annealing of Tl_2S-Sb_2S_3 in oven for 2hours at 180^{o}C a ternary compound $TlSbS_2$ films was produced with band gap of 1.70 eV. This film shows good crystal structure as confirmed from XRD and photomicrograph. The direct-allowed transition is the most probable type of transition near the fundamental edge of Sb_2S_3, Tl_2S and $TlSbS_2$ films. The calculated values of E_g for the films are close to the reported values of the thin films. The refractive index and real part of dielectric constant increase with the decreasing photon energy. The refractive index values have been fitted to the single-oscillator models. The values obtained for the single-oscillator energy E_o are consistent with the optical gap results. Because the films have low of band gap and show poor transmission of visible light they could find potential applications as solar cell absorbers.

References

[1] R. S. Mane, C. D. Lokhande, Mater. Chem. Phys. **65**, 1 1(2000)
[2] V. Janickis, I. Ancutienė, I. Bružaitė, and V. Jasulaitienė, Mat. Sci. **10**, 3 231 (2004)
[3] V. Gopal and J. A. Harrington, Opt. Express **11**, 24 3182 (2003)
[4] V. Estrella, M. T. S. Nair, and P. K. Nair, Thin Solid Films, **414**, 281 (2002).
[5] K. C. Mandal and A. Mondal, J. Phys. Chem. Solids, **51**, 339 (1990)
[6] J. George and M. K. Radhakrishnan, Solid State Commun., **33**, 987 (1980).
[7] J. Grigas, J. Meshkauskas, and A. Orliukas, Phys. Status Solidi A, **37**, K39 (1976)
[8] M. S. Ablova, A. A. Andreev, T. T. Dedegkaev, B. T. Melekh, A. B. Peutsov, N. S. Shendel, L. N. Shumilova, Sov. Phys. Semicond., **10**, 629 (1976)
[9] K. H. A. Mady, M. M. El-Nahas, A. M. Farid, and H. S. Soliman, J. Mater. Sci., **23**, 3636 (1988).
[10] M. T.S. Nair, Y. Peña, J. Campos, V. M. Garcia, P. K. Nair J. Electrochem. Soc., **145** (6), (1998).
[11] Y. Rodríguez-Lazcano, L. Guerrero, O.Gomez Daza, M. T. S. Nair, P. K. Nair Superficies y Vacío **9**, 100, 1999
[12] P. K. Nair, M. T. S. Nair, A. Fernandez and M.Ocampo, J. Phys. D: Appl. Phys. **22**, 829 (1989)
[13] M. T. S. Nair, Y. Peña, J. Campos, V. M. García and P. K. Nair, J. Electrochem. Soc. **145**, 2113 (1998)
[14] S. M. Sze, Physics of semiconductor Devices, (Wiley, New York, 1981), p.849 and 751
[15] Verónica Estrella, Rogelio Mejía, M. T. S. Nair, P. K. Nair, Mod. Phys. Lett. B, **15**(17-19), 737 (2001)
[16] Semiconductors other that Group IV Elements and III-V Compounds, Data in Science and Technology, edited by O. Madelung, (Springer-Verlag, Berlin, 1992) , p.149.

[17] V. Estrella, M. T. S. Nair, and P. K. Nair, Semicond. Sci. Technol., **17**, 119 (2002)
[18] J. Tauc, R. Grigorovici, A. Vancu, Phys. Stat. Sol. **15**, 627(1966)
[19] V. Estrella, M.T.S. Nair and P.K. Nair. Mater. Res. Soc. **722** K9.10.1 (2002)
[20] F.I. Ezema, J. Research (Sci.) **15** (4), 343(2004)
[21] F.I. Ezema, Turk. J. Phys. **29**, 105(2005)
[22] F.I. Ezema, Pacific Journ. Sci. and Technol. **6** (1), 6(2005)
[23] F.I. Ezema and M.N. Nnabuchi, Discovery and Innovation**, 17**(3&4), 156 (2005)
[24] F.I. Ezema and M.N. Nnabuchi, Journal Appl. Sci. and Technol. **10**(1&2), 53(2005)
[25] F.I. Ezema and A.B.C. Ekwealor, Nig. Journ. Sol. Ener., **15**, 73(2005)
[26] F.I. Ezema and M.N. Nnabuchi, J. Res. (Sci.), **17**(2), 115(2006)
[27] F.I. Ezema, A.B.C. Ekwealor and R.U. Osuji, Turk. Journ. Phys., **30**, 157(2006)
[28] F.I. Ezema and R.U. Osuji, Journ. Appl. Sci., 6(8), 1827(2006)
[29] F.I. Ezema, M.N. Nnabuchi and R.U. Osuji, Trends Appl. Sci. Res. **1**(5), 467(2006)[23]see, e.g., N.F. Mott, E.A. Davis, Electronic Processes in Non-Crystalline Materials, (Clarendon Press, Oxford, 1979)
[30] K. L. Chopra, B. C. Kainthla, D. K. Pandya, and A. P Thakoor, in Physics of Thin Films, Edited by G. Hass, M. H. Francombe, and J. L. Vossen, Vol. 12, (Academic Press, New York 1982) pp. 201,
[31] A. Arias-Carbajal Readigos, V.M. Gearcıa, O. Gomezdaza, J. Campos, M.T.S. Nair, P.K. Nair, Semicond. Sci. Technol. **15**, 1022(2000)
[32] I.M.Tsidilkovsk, Band structure of semiconductors, Pergamon Press, Oxford (1982)
[33] J.I. Pankove, Optical processes in semiconductors, Prentice-Hall, New York (1971)
[34] R.A. Smith in Semiconductors, 2nd ed. (Cambridge University Press, Great Britain, 1978) pp. 309-326.

[35] A. Abu EL-Fadl, Galal A. Mohamad, A.B. Abd El-Moiz, M. Rashad Physica B **366**, 44(2005)
[36] I.C. Ndukwe, Sol. Ener. Mater. Sol. Cells, **40**, 123 (1996)
[37] Janai, M., D.D. Alfred, D.C. Booth and B.O. Seraphin, Sol. Ener. Mater. 1, 11(1979)
[38] S.H. Wemple, and M. Di Domenico, Phys. Rev. B 3, 1338(1971)
[39] S.H. Wemple, Phys. Rev. B 7, 3767(1973)
[40] K. Tanaka, Thin Solid Films 66, 271(1980)